Stick-Slip Dynamics of a Stressed Ion Crystal

T. B. Mitchell,[1] J. J. Bollinger,[2] W. M. Itano,[2] and D. H. E. Dubin[3]

[1]*Department of Physics and Astronomy, University of Delaware, Newark, Delaware 19716*
[2]*Time and Frequency Division, National Institute of Standards and Technology, Boulder, Colorado 80305*
[3]*Department of Physics, University of California at San Diego, La Jolla, California 92093*

(Received 24 May 2001; published 10 October 2001)

We study the control of the rotation of a laser-cooled ion crystal in a Penning trap by a rotating electric field perturbation. We show that application of a small torque produces sudden angular jumps or "slips" of the crystal orientation spaced by intervals when the crystal is phase locked or "stuck" relative to the rotating perturbation. The distribution of angular slips is described by a power law, where the power-law exponent depends on the applied torque. We believe this system is driven by a constant force and small perturbations or thermal effects trigger the slips.

Non-neutral plasmas confined in Penning-Malmberg traps are used in a variety of experiments including plasma physics [1], Coulomb crystal studies [2,3], precision spectroscopy [4], antimatter research [5], and storage of highly charged ions [6]. Recently there has been a great deal of interest in using a rotating electric field perturbation to control the global $\mathbf{E} \times \mathbf{B}$ rotation of these plasmas [5,7,8]. For crystallized ion plasmas, phase-locked control of the plasma rotation has been demonstrated [8], which has important implications for atomic clocks [4] and for quantum computation with trapped ions [9]. In this Letter we study the limits to phase-locked control due to the application of a small torque produced by the radiation pressure of a weak laser beam. We observe sudden angular jumps or "slips" of the crystal orientation spaced by intervals when the crystal orientation is phase locked or "stuck" relative to the rotating perturbation. Stick-slip behavior similar to that observed here is found in many different and diverse systems: for example, in studies of friction between two surfaces [10,11], in experiments on avalanches and slips in granular systems [12–14], and as the underlying process in spring-block models of earthquakes [15,16]. Many of these systems, including the study presented here, exhibit a power-law distribution of the slip amplitudes, indicative of an underlying critical point [17,18].

Our work uses the Penning-Malmberg trap at NIST to store $\sim 15\,000$ $^9\mathrm{Be}^+$ ions. The ions interact by unscreened Coulomb repulsion and are Doppler laser cooled [19] to millikelvin temperatures, where their thermal energy is small compared to the Coulomb potential energy between nearest neighbor ions. Under these conditions the ions are strongly coupled [20] and form a Coulomb crystal (a classical Wigner crystal) [2,3]. Structurally similar Coulomb crystals are believed to exist in dense astrophysical matter, such as the interior of white dwarfs and the outer crust of neutron stars [21]. Observations of power-law statistics of soft gamma-ray events have recently been interpreted as evidence that the Coulomb crystal comprising the outer crust of a magnetized neutron star can undergo very large-scale slips ("starquakes") [22,23]. The measured power-law exponents of the neutron starquakes lie within the range of exponents we measure here (see Fig. 3).

Figure 1(a) shows the experimental setup [3,8]. The $^9\mathrm{Be}^+$ ions were confined radially by a uniform magnetic field $B = 4.465$ T (cyclotron frequency $\Omega_c/2\pi = 7.608$ MHz) in the $\hat{z}$ direction and axially by a potential difference of $V_0 = -500$ V applied between the center and end electrodes of the trap. Near the trap center the trap
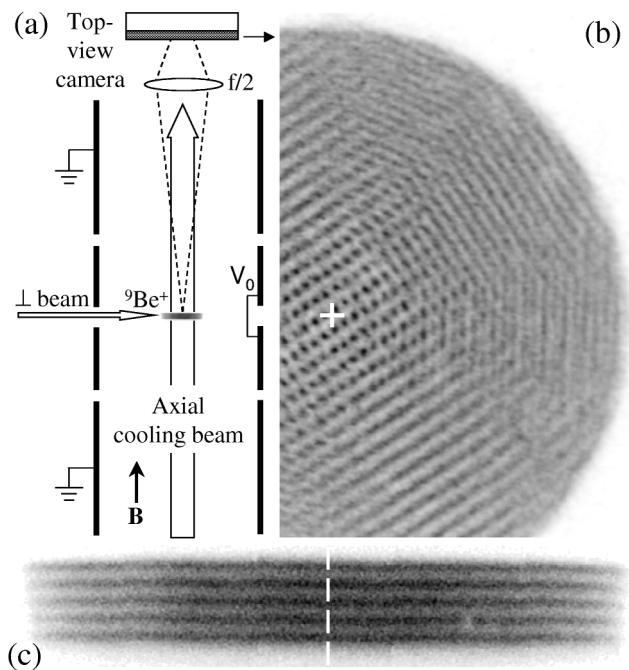

FIG. 1. (a) Schematic of the cylindrical Penning trap and the top-view imaging system. The side-view imaging system is not shown. (b) Strobed top-view image of a five-axial plane $^9\mathrm{Be}^+$ ion crystal with a bcc structure, similar to those used in this study. (c) Side-view image (unstrobed) of the same ion crystal. The diameter ($2r_{\mathrm{Be}}$) of the $^9\mathrm{Be}^+$ ions is 495 μm. Ions of greater mass are located at $r > r_{\mathrm{Be}}$ but do not fluoresce in the laser beam. The rotation axes are indicated.

potential is quadratic and given by $m\omega_z^2(z^2 - r^2/2)/(2e)$, where the axial frequency $\omega_z/2\pi = 565$ kHz for ^{9}Be$^+$. Here r and z denote the cylindrical radial and axial coordinates. Because of the axial magnetic field and the radial components of the ion space charge and trap electric fields, the ion crystal rotates at a frequency ω_r about the trap symmetry ($\hat{z}$) axis. In addition to ^{9}Be$^+$ ions, ions of greater mass ("heavy ions") such as BeH$^+$ and BeOH$^+$ are created by reactions with ^{9}Be$^+$ ions and background neutral molecules. For the work discussed here, typically 20% to 50% of the plasma consisted of heavy impurity ions. These ions are sympathetically cooled to temperatures similar to the ^{9}Be$^+$ ions and, due to the rotation, centrifugally separate to larger radii where they crystallize.

We applied an electric field perturbation rotating about the $\hat{z}$ axis at frequency ω_{rp} to control ω_r [8]. The rotating perturbation applies a torque on the radial boundary of the plasma (on the nonfluorescing, heavy ions) by creating a small-amplitude traveling wave. The torque due to this wave is then transferred to the plasma interior through the strong interparticle forces, which act to bring the plasma to the same rotation frequency as ω_{rp} [24]. We observe similar stick-slip motion with both dipole and quadrupole rotating fields. However, most measurements, including those we report here, were taken with a dipole rotating field. The radial binding force of the trap is due to the Lorentz force produced by the plasma's rotation through the magnetic field. Therefore, changing ω_r changes the radial binding force of the trap and provides a sensitive way to adjust the overall shape and structural phase of the plasma. In this work, $\omega_r \approx \omega_{rp} = 2\pi \times 22.8$ kHz, which produced a disk-shaped plasma consisting of five axial planes and a bcc-like crystal structure in the plasma center [3]. Because $\omega_r \ll \Omega_c$, the ion motion in a direction perpendicular to the magnetic field is determined principally by $\mathbf{E} \times \mathbf{B}$ guiding center dynamics [25].

The main cooling-laser beam ($\lambda = 313$ nm) was directed along the z axis. This beam's power was $\sim$50 μW, and it was focused to a $\sim$0.5 mm waist at the ion crystal. A second cooling beam [$\perp$ beam in Fig. 1(a)], derived from the same laser, was directed perpendicularly to $\hat{z}$ and had a $\sim$70 μm waist and $\sim$1 μW power. Both the perpendicular and parallel cooling lasers were required to form a well defined crystal in the disk-shaped plasmas discussed here. The $\perp$ beam is normally directed through the radial center ($r = 0$) of the crystal in order to minimize its applied torque while providing a low Doppler-cooling temperature [19]. In this experiment, we offset the $\perp$-beam position slightly (5–30 μm) from the plasma center to produce a torque on the ^{9}Be$^+$ ions in the same direction as the plasma rotation [26]. The torque from the $\perp$ beam was larger than any other ambient torque due to, for example, asymmetries in the trap construction or background gas drag.

A series of lenses formed side- and top-view images of the ion fluorescence, with viewing directions perpen-

dicular and parallel to the magnetic field, respectively, on either a gateable charge-coupled device (CCD) camera or an imaging photomultiplier tube. The resolution of the optical systems was $\sim$4 μm, while typical interparticle spacings were $\sim$15 μm. By detecting the ion fluorescence synchronously with the rotating perturbation drive, images of the individual ions which make up the Coulomb crystals were obtained. Figure 1(b) shows a strobed, top-view CCD camera image accumulated over 40 s of a five-axial plane crystal in the bcc structural phase. The ion positions are well localized in the plasma center; however, at larger radii they are blurred.

To investigate the blurring we used the imaging photomultiplier tube in the top-view position to record the positions and detection times of the fluorescence photons. Runs consisted of 125 ms intervals of data recorded each second over long periods of time (up to 5000 s). Images similar to those in Fig. 1(b) were created for each 125 ms interval by constructing 2D histograms of the ion fluorescence in the frame of the rotating perturbation. The orientation θ_{cry} of the central crystallized region in the rotating frame was determined (modulo π due to the bcc crystal bilateral symmetry) with an uncertainty of $\sim$0.002π rad [27].

In Fig. 2 we plot $\theta_{cry}(t)$ for two runs which differ mainly in the amount of $\perp$-beam torque. Over long time scales the $\perp$-beam torque produces a slightly faster rotation (a rotational "creep") of the ^{9}Be$^+$ crystal relative to the rotating perturbation. For example, in run 2 $\Delta\omega \equiv \omega_r - \omega_{rp} \approx 2\pi \times 8$ mHz. Over shorter time scales, as shown in the inset in Fig. 2, much of this crystal rotation takes place with sudden jumps in θ_{cry}, slips, whose time scale is too fast to be captured by the top-view diagnostic. Intermittent behavior appears to be a common feature in the plastic deformation (creep) of many materials. (See [28] for
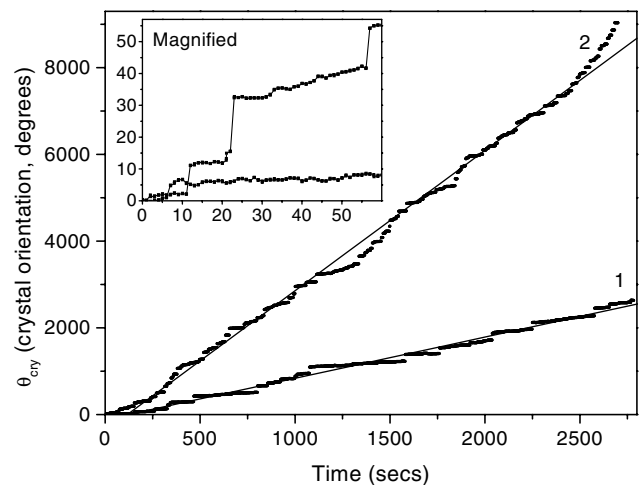
FIG. 2. Crystal orientation θ_{cry} in the frame of the rotating perturbation for two data runs with different $\perp$-beam torques. The torque is greater in run 2. The lines are from a linear regression fit. The inset shows a magnified plot of the first 60 s of data.

references.) Let $\Delta\theta_{cry}$ denote the angular displacement between two successive measurements of θ_{cry}. The statistics of $\Delta\theta_{cry}$ consists of a normal distribution (from measurement error) centered about zero with a width of $\sim 0.002\pi$, and infrequent larger slips. Because of the known sign of the $\perp$-beam torque and the π ambiguity mentioned above, we choose $\Delta\theta_{cry}$ to lie in the range $[0, \pi)$. To separate statistically significant slips from measurement error we further require $0.007\pi \leq \Delta\theta_{cry} \leq 0.97\pi$. We find that statistically significant slips account for greater than 90% of the measured change in θ_{cry}.

The $\perp$-beam torque is applied to all the $^9\text{Be}^+$ ions in the radial interior of the crystal. The rotating perturbation, however, applies its torque on the outer radial boundary of the heavy ions. We therefore believe the stress due to the competition between these torques is greatest in the region of the heavy ions and anticipate that the slips of Fig. 2 are due to ion motion between the radial boundary of the $^9\text{Be}^+$ ions, r_{Be}, and the overall radial boundary of the plasma. This is supported by the top-view images, which show most slips occurring as approximate rigid rotations of the $^9\text{Be}^+$ ions and also by simulation work discussed below. Because the slips occur at a radius greater than r_{Be}, and r_{Be} varied from run to run, we characterize a slip amplitude A_{slip} by the linear distance $\Delta\theta_{cry}r_{Be}$.

Figure 3 shows the distribution $f(A_{slip})$ of slips for the two data runs shown in Fig. 2. Because we cannot distinguish between slips with amplitude A_{slip} or $A_{slip} + n\pi r_{Be}$, where n is an integer, we fit to the function $f_{slip} \propto \sum_{n=0}^{n_{cut}}(A_{slip} + n\pi r_{Be})^{-\gamma}$ to determine the agreement of the data with a power-law distribution. Here n_{cut} is a cutoff that could depend on the system size, creep rate, or other factors. We obtain a good fit for
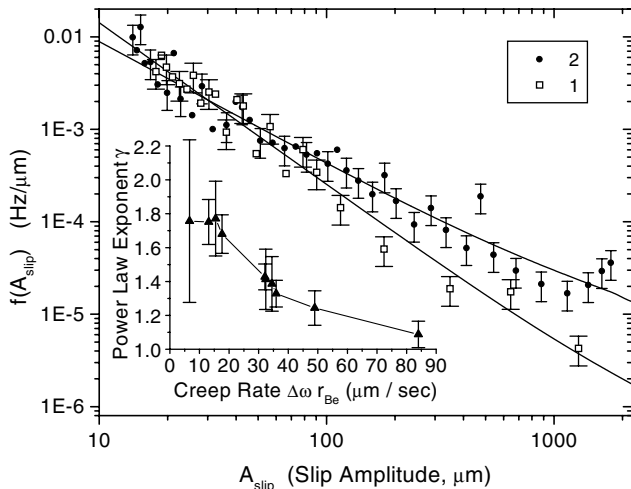

FIG. 3. Distribution $f(A_{slip})$, where $f(A_{slip})dA_{slip}$ is the frequency of slips between A_{slip} and $A_{slip} + dA_{slip}$, for the two data runs shown in Fig. 2. The lines are fits to a power law with a cutoff as described in the text. The inset shows the measured power-law exponent γ versus applied torque, as parametrized by the creep rate, for all of the data runs.

any n_{cut} but find that χ^2 goes through a weak minimum at $n_{cut} = 6$. We use $n_{cut} = 6$ in the following analysis. This results in measured γs slightly larger ($<$10% and within the uncertainty of the fit) than those resulting from $n_{cut} = 1$. In the inset in Fig. 3 we plot the measured power-law exponent γ as a function of the creep rate $\Delta\omega r_{Be}$ for ten data runs with the same rotating perturbation strength but different $\perp$-beam torques. We find that γ decreases as the creep rate, a measure of the applied $\perp$-beam torque, increases. Decreases in the stick-slip exponent with increased drive have been observed in some systems [11,29,30], but not in others [28].

Most experiments exhibiting stick-slip behavior are performed with "constant-velocity driving" where the force is applied through an effective elastic coupling [11–13]. The driving force of the system is something like $F(t) = K[Vt - x(t)]$, where "x" is the "position" of an element in the system (for example, the position of a bead or slider block in a chain), K is the effective spring constant coupling the applied force to each element in the system, and V is the constant average velocity that is imposed on the system. Stick-slip motion occurs for small V and K and a critical point exists in the limit $V \to 0$ and $K \to 0$ [18,29]. If the system gets stuck, it will eventually slip again because the driving force increases linearly until slip occurs. However, this experiment is performed under conditions more similar to "constant-force driving" since the $\perp$-beam radiation-pressure force is constant in time and applied directly to the $^9\text{Be}^+$ ions. In constant-force driving the system undergoes a depinning transition at a critical force F_c and moves with constant average velocity proportional to $(F - F_c)^\beta$ for $F > F_c$ and critical exponent β [29].

Inspection of Fig. 2 shows that the time intervals between successive slips (the waiting periods) are typically many seconds. An analysis of the waiting periods shows an approximately Gaussian distribution with mean waiting periods ranging from 4 s for the highest $\perp$-beam torques to 12 s for the lowest $\perp$-beam torques. These waiting periods are long compared to any known dynamical time scales due to internal modes of the system. In constant-force driving, if the system gets stuck for such a long period, it should permanently stick, which is not what we observe. One possibility is that the slips could be excited by a perturbation. By deliberately modulating the amplitude of the cooling and torquing lasers we have established that the amplitude noise present in these beams is not high enough to trigger slips.

We have performed molecular-dynamics simulations with 1000 ions (40% $^9\text{Be}^+$, 60% heavy) with the goal of better understanding the source of the slips. About four months of computation time has been required to simulate the equivalent of $\sim$1 s of experimental time. The simulations have produced one event which can be interpreted as a slip. In that event a rearrangement of a small number of heavy ions in the vicinity of a lattice defect produced a sudden change in the orientation of the

crystal. Because it appears that the rearrangement of a few heavy ions can trigger a slip, thermal fluctuations of the ions may be responsible for starting a slip. Once started, the slip eventually stops because the driving force of the $\perp$ beam is not sufficient to sustain continuous motion.

In summary, we have observed stick-slip motion in the rotational control of laser-cooled ion crystals in a Penning trap. We believe this system is constant-force driven and may be an experimental example of a subcritical state [18] where the slips are triggered by thermal fluctuations or by other unidentified perturbations (such as collisions with neutral background atoms). The trapped-ion crystal system discussed here possesses most of the features of a self-organized critical (SOC) state [17,18]. Therefore further investigations of the stick-slip behavior over a wider range of control parameters ($\perp$-beam torque, temperature, and rotating perturbation strength) could be useful for understanding the applicability of the SOC concept to real physical systems. Finally, minimizing the occurrence of the slips is important for some applications [4,9]. This can be done by minimizing the $\perp$-beam torque, either through active control of the $\perp$-beam position or by appropriate tailoring of the $\perp$-beam profile [31]. Increasing the strength of the rotating perturbation should also decrease the frequency of slips due to small ion rearrangements. Two runs taken with half the rotating perturbation strength of the data set analyzed here showed an increase in the number of slips and rotational creep of the ion crystal.

---

[1] *Non-Neutral Plasma Physics III,* edited by J. J. Bollinger, R. Spencer, and R. Davidson (AIP, New York, 1999).

[2] W. M. Itano, J. J. Bollinger, J. N. Tan, B. Jelenković, X.-P. Huang, and D. J. Wineland, Science **279**, 686 (1998).

[3] T. B. Mitchell, J. J. Bollinger, D. H. E. Dubin, X.-P. Huang, W. M. Itano, and R. H. Baughman, Science **282**, 1290 (1998).

[4] J. N. Tan, J. J. Bollinger, and D. J. Wineland, IEEE Trans. Instrum. Meas. **44**, 144 (1995).

[5] R. G. Greaves and C. M. Surko, Phys. Rev. Lett. **85**, 1883 (2000).

[6] L. Gruber, J. P. Holder, J. Steiger, B. R. Beck, H. E. DeWitt, J. Glassman, J. W. McDonald, D. A. Church, and D. Schneider, Phys. Rev. Lett. **86**, 636 (2001).

[7] E. M. Hollmann, F. Anderegg, and C. F. Driscoll, Phys. Plasmas **7**, 2776 (2000).

[8] X.-P. Huang, J. J. Bollinger, T. B. Mitchell, and W. M. Itano, Phys. Plasmas **5**, 1656 (1998).

[9] J. I. Cirac and P. Zoller, Phys. Rev. Lett. **74**, 4091 (1995).

[10] A. L. Demirel and S. Granick, Phys. Rev. Lett. **77**, 4330 (1996).

[11] S. Ciliberto and C. Laroche, J. Phys. I (France) **4**, 223 (1994).

[12] S. Nasuno, A. Kudrolli, and J. P. Gollub, Phys. Rev. Lett. **79**, 949 (1997).

[13] I. Albert, P. Tegzes, B. Kahnig, R. Albert, J. G. Sample, M. Pfeifer, A.-L. Barabási, T. Vicsek, and P. Schiffer, Phys. Rev. Lett. **84**, 5122 (2000).

[14] V. Frette, K. Christensen, A. Malthe-Sørenssen, J. Feder, T. Jøssang, and P. Meakin, Nature (London) **379**, 49 (1996).

[15] Z. Olami, H. J. S. Feder, and K. Christensen, Phys. Rev. Lett. **68**, 1244 (1992).

[16] R. Burridge and L. Knopoff, Bull. Seismol. Soc. Am. **57**, 341 (1967).

[17] P. Bak, C. Tang, and K. Wiesenfeld, Phys. Rev. Lett. **59**, 381 (1987).

[18] A. Vespignani and S. Zapperi, Phys. Rev. E **57**, 6345 (1998).

[19] W. M. Itano, L. R. Brewer, D. J. Larson, and D. J. Wineland, Phys. Rev. A **38**, 5698 (1988).

[20] S. Ichimaru, H. Iyetomi, and S. Tanaka, Phys. Rep. **149**, 91 (1987).

[21] H. M. Van Horn, Science **252**, 384 (1991).

[22] B. Cheng, R. I. Epstein, R. A. Guyer, and A. C. Young, Nature (London) **382**, 518 (1996).

[23] E. Göğüş, P. M. Woods, C. Kouveliotou, J. van Paradus, M. S. Briggs, R. C. Duncan, and C. Thompson, Astrophys. J. **532**, L121 (2000).

[24] D. H. E. Dubin and T. M. O'Neil, Rev. Mod. Phys. **71**, 87 (1999).

[25] D. H. E. Dubin and T. M. O'Neil, Phys. Rev. Lett. **60**, 511 (1988).

[26] D. J. Wineland, J. J. Bollinger, W. M. Itano, and J. D. Prestage, J. Opt. Soc. Am. B **2**, 1721 (1985).

[27] The crystal images occasionally showed defect lines that moved slowly across the crystal and prevented a definitive measurement of θ_{cry}. This occurred more frequently with larger torque. In this case shorter time series separated by intervals when θ_{cry} could not be unambiguously determined were appended to each other without introducing discontinuities in θ_{cry} at the junctures.

[28] M.-C. Miguel, A. Vespignani, S. Zapperi, J. Weiss, and J.-R. Grasso, Nature (London) **410**, 667 (2001).

[29] F. Lacombe, S. Zapperi, and H. J. Hermann, Phys. Rev. B **63**, 104104 (2001).

[30] S. Zapperi, P. Cizeau, G. Durin, and H. E. Stanley, Phys. Rev. B **58**, 6353 (1998).

[31] The $\perp$-beam torque can be reduced with a beam that has a large waist and frequency dispersion across the waist that matches the ion Doppler shifts due to the plasma rotation.